CLRC

The Dualized Standard Model and its Applications

Chan Hong-Mo   J Bordes and Tsou Sheung Tsun

14th October 1998

COUNCIL FOR THE CENTRAL LABORATORY OF THE RESEARCH COUNCILS

THE DUALIZED STANDARD MODEL AND ITS APPLICATIONS

CHAN Hong-Mo

Rutherford Appleton Laboratory, Chilton, Didcot, Oxon, OX11 0QX, United Kingdom
E-mail: chanhm @ v2.rl.ac.uk

José BORDES

Dept. Fisica Teorica, Univ. de Valencia, c. Dr. Moliner 50, E-46100 Burjassot (Valencia), Spain
E-mail: jose.M.bordes @ uv.es

TSOU Sheung Tsun

Mathematical Institute, University of Oxford, 24-29 St. Giles', Oxford, OX1 3LB, United Kingdom
E-mail: tsou @ maths.ox.ac.uk

The Dualized Standard Model offers a natural explanation for Higgs fields and 3 generations of fermions plus a perturbative method for calculating SM parameters. By adjusting only 3 parameters, 14 quark and lepton masses and mixing parameters (including ν oscillations) are calculated with general good success. Further predictions are obtained in post-GZK air showers and FCNC decays.

In this article, we summarize some work which has occupied us for some years. The material has been summarized in 5 papers submitted to this conference (Papers 607, 610, 611, 613, 636), and this talk is but a summary of these summaries.

The Dualized Standard Model [1] is a scheme which aims to answer some of the questions left open by the Standard Model (such as why Higgs fields or fermion generations should exist) and to explain the values of some the Standard Model's many parameters (such as fermion masses and mixing angles). In contrast to most schemes with similar aims, the DSM remains entirely within the Standard Model framework, introducing neither supersymmetry nor higher space-time dimensions. That it is able to derive results beyond the Stardard Model while remaining within its framework is by exploiting a generalization of electric-magnetic duality to nonabelian Yang-Mills theory found a couple of years ago [2].

The concept of duality is best explained by recalling the well-known example in electromagnetism. There a dual transform (the Hodge star) is defined: $^*F_{\mu\nu} = -(1/2)\epsilon_{\mu\nu\rho\sigma}F^{\rho\sigma}$, where for both the Maxwell field $F_{\mu\nu}$ and its dual $^*F_{\mu\nu}$ potentials A_μ and $\tilde{A}_\mu$ exist, so that the theory is invariant under both A_μ and $\tilde{A}_\mu$ gauge transformations. The theory has thus in all a $U(1) \times \tilde{U}(1)$ gauge symmetry with $U(1)$ corresponding to electricity and $\tilde{U}(1)$ to magnetism. Magnetic charges are monopoles in $U(1)$, while electric charges are monopoles of $\tilde{U}(1)$.

The same statements do not hold for nonabelian Yang-Mills theory under the dual transform [3] (star). However, it was shown [2] that there exists a generalized dual transform for which similar results apply. Its exact

form, in the language of loop space [4,5], need not here bother us. What matters, however, is that given this generalized transform, a potential can again be defined for both the Yang-Mills field and its dual, and that the theory is invariant under both the gauge transformations:

$$A_\mu \to A_\mu + \partial_\mu\Lambda + ig[\Lambda, A_\mu], \ \tilde{A}_\mu \to \tilde{A}_\mu + \partial_\mu\tilde{\Lambda} + i\tilde{g}[\tilde{\Lambda}, \tilde{A}_\mu],$$
$$(1)$$

with $g, \tilde{g}$ satisfying the (generalized) Dirac quantization condition [6]: $g\tilde{g} = 4\pi$. As a result, the theory has in all the gauge symmetry $SU(N) \times \widetilde{SU}(N)$ with $SU(N)$ corresponding to (electric) 'colour' and $\widetilde{SU}(N)$ to (magnetic) 'dual colour'. And again, dual colour charges are monopoles in $SU(N)$, while colour charges appear as monopoles in $\widetilde{SU}(N)$ [7].

Applied to colour in the Standard Model, this nonabelian duality [2] gives two new interesting features. First, dual to the $SU(3)$ symmetry of colour, the theory possesses also an $\widetilde{SU}(3)$ symmetry of dual colour. Then, by a well-known result of 't Hooft [8], since colour is confined, it follows that this $\widetilde{SU}(3)$ of dual colour has to be broken via a Higgs mechanism[a]. Hence, the theory already contains within itself a broken 3-fold gauge symmetry which could play the role of the 'horizontal' symmetry wanted to explain the existence in nature of the 3 fermion generations. Second, in the generalized dual transform [2], the frame vectors ('dreibeins') in the gauge group take on a dynamical role [7] which suggests that they be promoted to physical fields. If so, then they possess the properties

---

[a]It has been shown [6] the duality introduced [2] indeed satisfies the commutation relations of the order-disorder parameters used by 't Hooft to define his duality.

that one wants for Higgs fields for symmetry breaking (as in electroweak theory): space-time scalars belonging to the fundamental representation having classical values (vev's) with finite lengths.

The basis of the Dualized Standard Model is just in making this bold assumption of identifying the dual colour $\widetilde{SU}(3)$ as the 'horizontal' generation symmetry and of the frame vectors in it as the Higgs fields for its breaking. We note that according to nonabelian duality [2], the niches already exist in the original theory in the form of the dual symmetry and the 'dreibeins'. One could thus claim that the DSM offers an explanation for the existence both of exactly 3 fermion generations and of Higgs fields necessary for breaking this generation symmetry.

This identification further suggests the manner in which the symmetry ought to be broken. As a result, the fermion mass matrix at tree-level takes the form [1]:

$$m = m_T \begin{pmatrix} x \\ y \\ z \end{pmatrix} (x, y, z), \qquad (2)$$

where m_T is a normalization factor depending on the fermion-type T, namely whether U- or D-type quarks, charged leptons (L) or neutrinos (N), and x, y, z are vacuum expectation values of Higgs fields (normalized for convenience: $x^2 + y^2 + z^2 = 1$), which are independent of the fermion-type T. Because m is factorizable it has only one nonzero eigenvalue so that at tree-level there is only one massive generation (fermion mass hierarchy). Further, because (x, y, z) is independent of the fermion-type, the state vectors of, say, the U- and D-type quarks in generation space have the same orientation, so that the CKM matrix is the unit matrix. These are already not a bad first approximation to the experimental situation.

One can go further, however. With loop corrections, it is seen that the mass matrix m' remains factorizable [1], with the same form as (2), but the vector (x', y', z'), in which the relevant information of m' is encoded, now rotates with the energy scale, tracing out a trajectory on the unit sphere. Hence, the lower generation fermions acquire small finite masses via 'leakage' from the highest generation. Furthermore, the vector (x', y', z') depends now on the fermion-type, giving rise to a nontrivial CKM matrix. The result is a perturbative method for calculating fermion mass and mixing parameters.

In a 1-loop calculation [9,10] it is found that out of the many diagrams only the Higgs loop diagram dominates, involving thus only a few adjustable parameters. The present score is as follows. By adjusting 3 parameters, namely a Yukawa coupling strength ρ and the 2 ratios between the Higgs vev's x, y, z, one has calculated the following 14 of the 'fundamental' SM parameters:

- the 3 parameters of the quark CKM matrix $|V_{rs}|$,
- the 3 parameters of the lepton CKM matrix $|U_{rs}|$,

Table 1: Fermion Masses

	$Calculation$	$Experiment$
m_c	1.327GeV	1.0 − 1.6GeV
m_s	0.173GeV	100 − 300MeV
m_μ	0.106GeV	105.7MeV
m_u	235MeV	2 − 8MeV
m_d	17MeV	5 − 15MeV
m_e	7MeV	0.511MeV
m_{ν_1}	10^{-15}eV	< 10eV
B	400TeV	?

- $m_c, m_s, m_\mu, m_u, m_d, m_e,$
- the masses m_{ν_1} of the lightest and B of the right-handed neutrinos,

there being no CP-violation at 1-loop order.

First, for the quark CKM matrix $|V_{rs}|$, where $r = u, c, t$ and $s = d, s, b$, one obtains for a sample fit [11]:

$$|V_{rs}| = \begin{pmatrix} 0.9752 & 0.2215 & 0.0048 \\ 0.2210 & 0.9744 & 0.0401 \\ 0.0136 & 0.0381 & 0.9992 \end{pmatrix}, \qquad (3)$$

as compared with the experimental values [12]:

$$\begin{pmatrix} 0.9745 - 0.9760 & 0.217 - 0.224 & 0.0018 - 0.0045 \\ 0.217 - 0.224 & 0.9737 - 0.9753 & 0.036 - 0.042 \\ 0.004 - 0.013 & 0.035 - 0.042 & 0.9991 - 0.9994 \end{pmatrix}. \qquad (4)$$

All the calculated values are seen to lie roughly within the experimental bounds.

Second, for the lepton CKM matrix $|U_{rs}|$, one obtains with the *same* 3 input parameters:

$$|U_{rs}| = \begin{pmatrix} 0.97 & 0.24 & 0.07 \\ 0.22 & 0.71 & 0.66 \\ 0.11 & 0.66 & 0.74 \end{pmatrix}, \qquad (5)$$

where $r = e, \mu, \tau$ and $s = 1, 2, 3$ label the physical states of the neutrinos. The empirical values of $|U_{rs}|$ for leptons are much less well-known. Collecting all the information so far available from neutrino oscillation experiments, one arrives at the following tentative arrangement:

$$|U_{rs}| = \begin{pmatrix} \star & 0.4 - 0.7 & 0.0 - 0.15 \\ \star & \star & 0.45 - 0.85 \\ \star & \star & \star \end{pmatrix}. \qquad (6)$$

which is seen to be in very good agreement with the prediction (5) for U_{e3} and $U_{\mu3}$, but not for U_{e2}.

Lastly, from the *same* calculation with the *same* 3 parameters, one obtains the fermion masses listed in Table 1. The second generation masses agree very well with experiment. Those of the lowest generation were obtained by extrapolation on a logarithmic scale and should

be regarded as reasonable if of roughly the right magnitude. As for the 2 neutrino masses, the experimental bounds are so weak that there is essentially no check.

In summary, out of the 14 quantities calculated, 8 are good ($|V_{rs}|, |U_{\mu3}|, |U_{e3}|, m_c, m_s, m_\mu$), 2 are reasonable ($m_d, m_e$), 2 are unsatisfactory ($|U_{e2}|, m_u$), and 2 are untested, which is not a bad score for a first-order calculation with only 3 parameters.

One interesting feature for the calculation outlined above is that the trajectories traced out by the vector (x', y', z') for the 4 different fermion-types U, D, L, N all coincide to a very good approximation, only with the 12 physical fermion states at different locations (Figure 1). The points $(1, 0, 0)$ and $\frac{1}{\sqrt{3}}(1, 1, 1)$ are fixed points so that
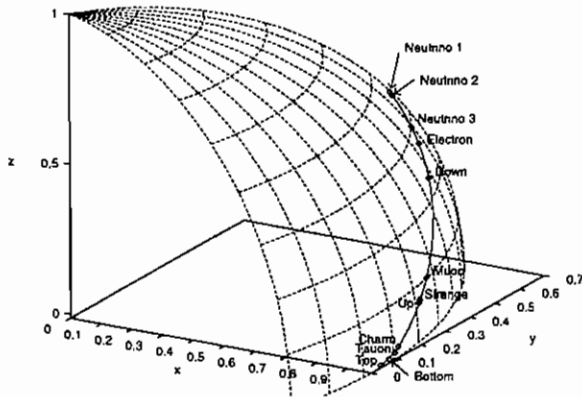

Figure 1: The trajectory of (x', y', z') as the energy scale varies.

the rate of flow is slower near the ends of the trajectory than in the middle. For this reason, the states t and b are close together in spite of their big mass difference. This observation will be of relevance later.

Since neutrino oscillations[13] are of particular interest at this conference, let us take a closer look[10]. The element $U_{\mu3}$ of the lepton CKM matrix giving the mixing between the muon neutrino ν_μ and the heaviest neutrino ν_3 is constrained mainly by the data on atmospheric neutrinos. From the old Kamiokande data[14] an analysis by Giunti et al.[15] gives the bounds on $U_{\mu3}$ shown in Figure 2. In the DSM scheme, with parameters already fixed by the fit to the quark sector[9], the elements of $|U_{rs}|$ are calculable given the masses of ν_3 and ν_2. Then, with m_{ν_2} taken in the range $10^{-11}\text{eV}^2 < m_2^2 < 10^{-10}\text{eV}^2$ as suggested by the Long Wave-Length Osicillation (LWO) (or the 'vacuum' or 'just-so') solution to the solar neutrino problem[16,17], the predicted band of values of $|U_{\mu3}|$ for a range of input values of m_{ν_3} is shown in Figure 2, passing right through the middle of the allowed region. No similar detailed analysis of the new SuperKamiokande data[13] has yet been performed, but the predicted band can be seen to remain well within the allowed region:
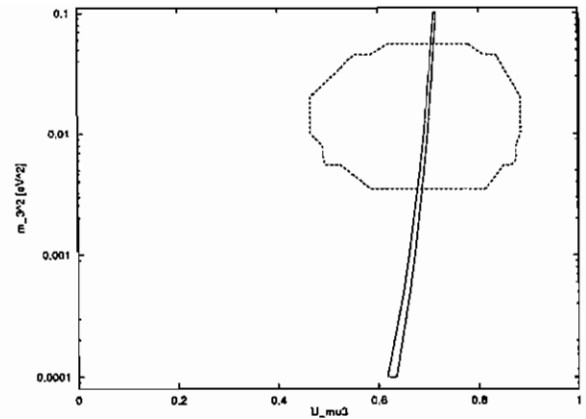

Figure 2: 90 % CL limits on $U_{\mu3}$ compared with DSM calculation.

$.53 < U_{\mu3} < .85$, $5 \times 10^{-4} < m_3^2 < 6 \times 10^{-3}\text{eV}^2$.

The same calculation gives the prediction shown in Figure 3 for the element U_{e3} representing the mixing between the electron neutrino ν_e and ν_3, which is constrained mainly by the reactor data from CHOOZ[18] and Bugey[19]. If m_3^2 is higher than $2 \times 10^{-3}\text{eV}^2$, as favoured by the old Kamiokande data[14,15] and the new data from Soudan reported in this conference[20], then the negative result from CHOOZ restricts U_{e3} to quite small values, as indicated in Figure 3 and quoted in (6). The new Su-
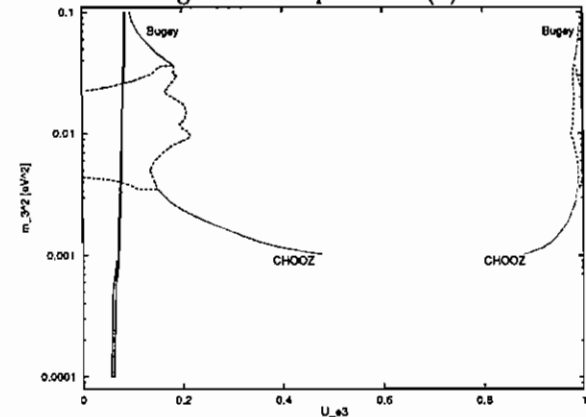

Figure 3: 90 % CL limits on U_{e3} compared with DSM calculation.

perKamiokande data[13] gives a best-fit value for m_3^2 of 2.2×10^{-3}, still implying by CHOOZ a small value for U_{e3}, but do not exclude lower values of m_3 and hence much larger values of U_{e3}. In any case, as seen in Figure 3, the band of values predicted by the DSM calculation falls always comfortably within the allowed region.

The DSM results summarized above for neutrino oscillations were obtained assuming m_2^2 of order 10^{-11} to 10^{-10}eV^2, as suggested by the LWO solution[16,17]. The alternative MSW[21] solutions for solar neutrinos require[22] $m_2^2 \sim 10^{-5}\text{eV}^2$, for which no sensible DSM solution was found[10]. It is thus intriguing to hear in this conference that the new SuperKamiokande data on the day-night variation and energy spectrum of solar neutrinos[13] also favours the LWO solution.

3

Further, generation being identified with dual colour in DSM, one expects only 3 generations of neutrinos. Thus, the result from Karmen [23] reported in this conference against the existence of another neutrino with mass of order eV, as previously suggested by the LSND experiment [24], is also in the DSM's favour.

It is particularly instructive to compare the CKM matrices for leptons and quarks. Both the empirical (4), (6) and the calculated (3), (5) matrices show the following salient features:

- that the 23 element for leptons is much larger than that for quarks,
- that the 13 elements for both quarks and leptons are much smaller than the rest,
- that the 12 element is largish and comparable in magnitude for quarks and leptons.

These features, all so crucial for interpreting existing data, not only are all correctly reproduced by DSM calculation, but also can be understood within the scheme using some classical differential geometry as follows [25].

First, it turns out [1,9] that in the limit when the separation between the top 2 generations is small on the trajectory traced out by (x', y', z'), which is the case for all 4 fermion-types as seen in Figure 1, then the vectors for the 3 generations form a Darboux triad [26] composed of (i) the radial vector (x', y', z') for the heaviest generation, (ii) the tangent vector to the trajectory for the second generation, and (iii) the vector normal to both the above for the lightest generation. The CKM matrix is thus just the matrix which gives the relative orientation between the Darboux triads for the two fermion-types concerned. Secondly, by the Serret–Frenet–Darboux formulae, it follows that the CKM matrix can be written, to first order in the separation Δs on the trajectory between t and b for quarks and between τ and ν_3 for leptons, as

$$CKM \sim \begin{pmatrix} 1 & -\kappa_g \Delta s & -\tau_g \Delta s \\ \kappa_g \Delta s & 1 & \kappa_n \Delta s \\ \tau_g \Delta s & -\kappa_n \Delta s & 1 \end{pmatrix}, \qquad (7)$$

where κ_n and κ_g are respectively the normal and geodesic curvature and τ_g is the geodesic torsion of the trajectory. Lastly, for our case of a curve on the unit sphere, $\kappa_n = 1$ and $\tau_g = 0$, from which it follows that :

- the 23 element equals roughly Δs,
- the 13 element is of second order in Δs,
- the 12 element depends on the details of the curve.

In Figure 1, Δs between τ and ν_3 is much larger than that between t and b, hence also the 23 element of the CKM matrix. Indeed, measuring the actual separations in Figure 1, one obtains already values very close to the actual CKM matrix elements in (3) and (5) or in (4) and (6). The 13 elements should be small in both cases, as already noted. As for the 12 elements, they depend on both the locations and details of the curve, which

explains why they need not differ much between quarks and leptons in spite of the difference in separation, and also why the DSM prediction in (5) is not as successful for this element as for the others.

To test DSM further, one seeks predictions outside the Standard Model framework. These are not hard to come by. Identifying generation to dual colour, which is a local gauge symmetry, makes it imperative that any particle carrying a generation index can interact via the exchange of the dual colour gauge bosons, leading to flavour-changing neutral current (FCNC) effects. Given the calculations on the CKM matrices outlined above, all low energy FCNC effects can now be calculated in terms of a single mass parameter ζ related to the vev's of the dual colour Higgs fields [27]. Inputting the mass difference $K_L - K_S$ which happens to give the tightest bound on $\zeta \sim 400\text{TeV}$, one obtains bounds on the branching ratios of various FCNC decays. In the following paragraph, an argument will be given which converts these bounds into actual order-of-magnitude estimates. In particular, the mode $K_L \to \mu^\pm e^\mp$ has a predicted branching ratio of around 10^{-13}, less than 2 orders away from the new BNL bound of 5.1×10^{-12} reported in this conference [28].

Since neutrinos carry a generation index, it follows that they will also acquire a new interaction through the exchange of dual colour bosons. At low energy, this interaction will be very weak, being suppressed by the large mass parameter ζ. However, at C.M. energy above ζ, this new interaction will become strong. With an estimate of at least 400TeV, the predicted new interaction is not observable in laboratory experiments at present or in the foreseeable future, but it may be accessible in cosmic rays. For a neutrino colliding with a nucleon at rest in our atmosphere, 400 TeV in the centre of mass corresponds to an incoming energy of about 10^{20}eV. Above this energy, neutrinos could thus in principle acquire a strong interaction and produce air showers in the atmosphere. Now air showers at and above this energy have been observed. They have long been a puzzle to cosmic ray physicists since they cannot be due to proton or nuclear primaries which would be quickly degraded from these energies by interaction with the 2.7 K microwave background [29]. Indeed, the GZK cutoff [30] for protons is at around $5 \times 10^{19}\text{eV}$. Neutrinos, on the other hand, are not so affected by the microwave background. Hence, if they can indeed produce air showers via the new interaction predicted by the DSM, they can give a very neat explanation for the old puzzle of air showers beyond the GZK cut-off [31]. Further tests for the proposal have been suggested [32]. The proposal also gives a rough upper bound on the mass parameter ζ governing FCNC effects which is close to the lower bound obtained in the preceding paragraph. It was on the basis of this coincidence that the above FCNC bounds were converted into

actual order-of-magnitude estimates.

The conclusions are summarized in Figure 4.

It is a pleasure for us to acknowledge our profitable and most enjoyable collaboration with Jacqueline Faridani and Jakov Pfaudler. TST also thanks the Royal Society for a travel grant to Vancouver.

References

1. Chan Hong-Mo and Tsou Sheung Tsun, Phys. Rev. D57, 2507, (1998).
2. Chan Hong-Mo, Jacqueline Faridani, and Tsou Sheung Tsun, Phys. Rev. D53, 7293, (1996).
3. CH Gu and CN Yang, Sci. Sin. 28, 483, (1975); TT Wu and CN Yang, Phys. Rev. D12, 3843 (1975).
4. A.M. Polyakov, Nucl. Phys. 164, 171, (1980).
5. Chan Hong-Mo and Tsou Sheung Tsun, *Some Elementary Gauge Theory Concepts* (World Scientific, Singapore, 1993).
6. Chan Hong-Mo and Tsou Sheung Tsun, Phys. Rev. D56, 3646, (1997).
7. Chan Hong-Mo, Jacqueline Faridani, and Tsou Sheung Tsun, Phys. Rev. D51, 7040 (1995).
8. G. 't Hooft, Nucl. Phys. B138, 1, (1978); Acta Phys. Austriaca. Suppl. 22, 531, (1980).
9. J Bordes, Chan H-M, J Faridani, J Pfaudler, Tsou ST, Phys. Rev. D58, 013004, (1998)
10. José Bordes, Chan Hong-Mo, Jakov Pfaudler, Tsou Sheung Tsun, Phys. Rev. D58, 053003 (1998).
11. Chan Hong-Mo and Tsou Sheung Tsun, Acta Phys. Polonica, B28, 3041, (1997)
12. Particle Physics Booklet, (1996), RM Barnett et al., Phys. Rev. D54, 1, (1996); web updates.
13. SuperKamiokande data, presented by C McGrew, M Vagins, M Takita at ICHEP'98.
14. K.S. Hirata et al., Phys. Letters, B205, 416, (1988); B280, 146, (1992); Y. Fukuda et al. Phys. Letter B335, 237, (1994).
15. C Giunti, CW Kim, M Monteno, hep-ph/9709439.
16. V. Barger, R.J.N. Phillips, and K. Whisnant, Phys. Rev. Letters, 69, 3135, (1992).
17. PI Krastev, ST Petcov, PRL 72, 1960, (1994).
18. CHOOZ collaboration, M. Apollonio et al., Phys. Lett. B420, 397, (1997).
19. B. Ackar et al., Nucl. Phys. 434, 503, (1995).
20. Soudan II, presented by H Gallagher at ICHEP'98.
21. L Wolfenstein, Phys. Rev. D17, 2369, (1978); SP Mikheyev, AYu Smirnov, Nuo. Cim. 9C, 17 (1986).
22. For example see G.L. Fogli, E. Lisi, and D. Montanino, Phys. Rev. D54, 2048 (1995).
23. Karmen, presented by J Kleinfeller at ICHEP'98.
24. C Athanassopoulos et al, PRL 75, 2650 (1995).
25. José Bordes, Chan Hong-Mo, Jakov Pfaudler, Tsou Sheung Tsun, Phys. Rev. D58, 053006 (1998).
26. See e.g. L.P. Eisenhart, *A Treatise on the Differential Geometry of Curves and Surfaces*, Ginn and Company 1909, Boston.
27. J Bordes, Chan H-M, J Faridani, J Pfaudler, Tsou ST, hep-ph/9807277, (1998).
28. BNL data in review by D Bryman at ICHEP'98.
29. Murat Boratav, astro-ph/9605087, Proc. 7th Int. Workshop on Neutrino Telescopes, Venice 1996.
30. K Greisen, PRL 16 (1966) 748; GT Zatsepin and VA Kuz'min, JETP Letters, 4 (1966) 78.
31. J Bordes, Chan HM, J Faridani, J Pfaudler, Tsou ST, hep-ph/9705463; hep-ph/9711438, to appear in Proc. of the Int. Workshop on Physics Beyond the Standard Model (1997) Valencia.
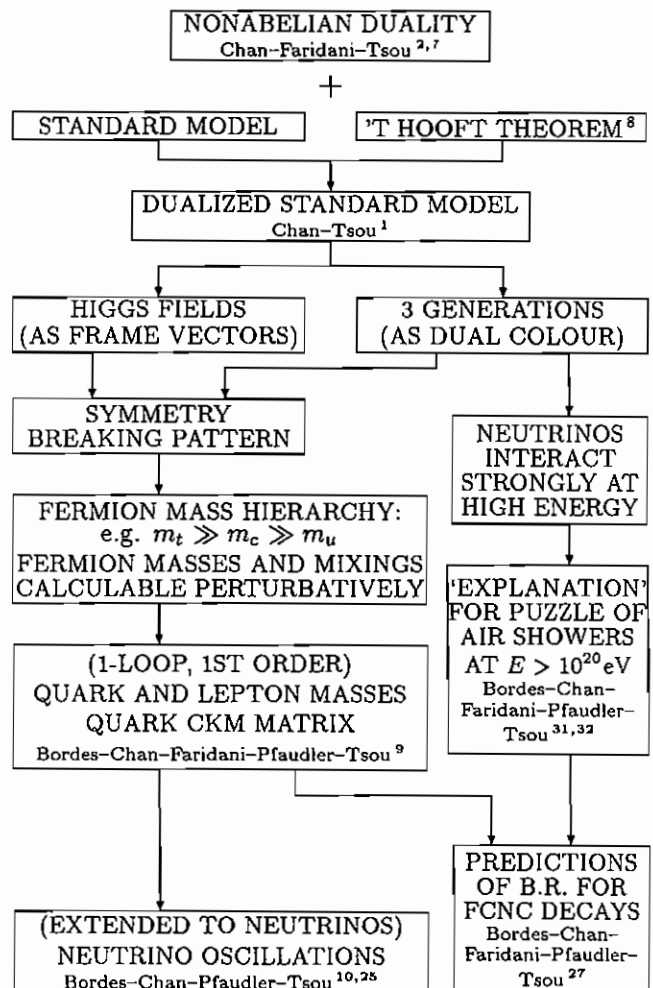32. J Bordes, Chan HM, J Faridani, J Pfaudler, Tsou ST, Astroparticle Phys. J., 8, 135 (1998).

Figure 4: Summary flow-chart